64-11

AFCRL - 64 - 145

Dr. Wolfram Bitterlich
I n n s b r u c k, Austria

To
European Air Research Office, Contracting Officer
American Embassy
Brussels, Shell Building, 47 Rue Cantersteen

Contract 61(052)-490

Date: 1 December 1963

(Dr. W. Bitterlich)

Technical Note No. 7

Research on: Propagation of VLF waves in liquid and solid media.

The research reported in this document has been sponsored by the United States Government.

Title of the technical note: Propagation of VLF waves in highly conducting medium, by O. Gröbner

Propagation of VLF waves in highly conducting medium

For studying the propagation of VLF waves in rock, an excursion to German and Dutch mines was made in September 1963. It was the purpose of this excursion to conduct measurements of subsurface propagation through geological bodies which in their structure and in the type of disturbances (mineralization) differed considerably from the regions of Tyrolian mines studied so far.

In the present report, interesting and informative results of measurements in one mine are discussed.

1. Theoretical considerations

According to the theory developed in the second Annual VLF Report (1962), which holds for a magnetic dipole in an unbounded and conducting medium, the magnetic field strength was calculated as dependent on the distance r, the angle φ and the conductivity σ. Below, the quantity Δ (see p 17, expression 40 and 41 in the above report) instead of the conductivity σ shall be considered to make the calculation more general, otherwise the results would be bound to a certain measuring frequency, but this is to be avoided. For this purpose, the function $h(r, \varphi, \Delta)$ (expression 52 of the report) was calculated for a number of distances and conductivities.

The function

$$h(r,\varphi,\Delta) = \frac{\exp(-\Delta r)}{r}\left\{\frac{4\cos^2\varphi}{r^2}\left(\frac{1}{r^2}+\frac{2\Delta}{r}+2\Delta^2\right)+\right.$$
$$\left.+\sin^2\varphi\left(\frac{1}{r^4}+\frac{2\Delta}{r^3}+\frac{2\Delta^2}{r^2}+\frac{4\Delta^2}{r}+4\Delta^2\right)\right\}^{1/2} \qquad (1)$$

is calculated in Table I for the values $\Delta = 4.86\cdot10^{-2}$; $1.085\cdot10^{-2}$; $3.45\cdot10^{-2}$; $7.7\cdot10^{-2}$; $1.09\cdot10^{-1}$. For the frequency 3kc/sec used for these measurements, the conductivity would be $\sigma = 10^{-2}$; 10^{-1}; $2\cdot10^{-1}$, $5\cdot10^{-1}$,

$1(\Omega^{-1}\cdot m^{-1})$. The graphical representations shown in Figs. 1 through 4 give a good illustration of the directional pattern as dependent on the distance at constant conductivity on the one hand, and at a given distance as dependent on the conductivity on the other hand. For a better survey, the value of the function $h(r,\vartheta,\Delta)$ was plotted in the diagram in radial direction (logarithmic scale). Fig. 3 clearly shows the result obtained previously, namely that the field strength component H_ϑ (in the direction $\vartheta = 90^\circ$) for a certain conductivity has a maximum at a given distance and frequency.

The definition of the function $\varphi(r,\Delta)$ in the form

$$\varphi(r,\Delta) = \frac{|H|_{\vartheta = 0^\circ}}{|H|_{\vartheta = 90^\circ}} \qquad (2)$$

proved advantageous for further studies. Table 2 gives some computed values of this function which are plotted in Fig. 5. By means of this function which on the whole is consistent with the function $V(r)$ in the report (see p. 16, expression 53), the conductivity can be determined from the value of $\varphi(r,\Delta)$ which can easily be measured by experiment, and from Fig. 5, via Δ. The considerable decrease of the value of the function characterizing the far field of the dipole indicates the predominance of the component H_ϑ.

In the present report it shall not be discussed how far the boundary of the medium can be neglected and how great the error thus becomes, since the existing results at present are being compared with the experimental data.

2. Measurements in the Salzgitter mine (Germany) - shaft region Konrad I

The geological structure of this region is characterized by a variety of flat strata formed by repeated flooding by the sea. The exploitable iron ore field of the Upper Jurassic is accompanied by zones of marly limestone. The rock on top of the mine has an average

height of 1000 m, the inclination of the deposit to the horizon being 22°. The concentration of this colitic ore is approximately 30%, the average size of the individual brown iron grains is 0.5 mm.

Suitable measuring sites with specific conditions in the mine itself were not easy to find. Regions with wires of the mining railway, power cables, or even iron formwork had to be avoided. Two short drifts 18 and 25 m long in the 1000 m bed seemed to be most suitable. Despite the short distance between transmitter and receiver, characteristic antenna patterns could be measured owing to the high conductivity of the ore body - a d-c measurement yielded $\sigma = 2 \cdot 10^{-1} (\Omega^{-1} m^{-1})$. The working method for finding these diagrams had already been described in detail in the above annual report. The transmitter antenna is successively turned into the positions $\alpha = 0°$, 30°, 60°, and 90°. In the meantime, measurements with the receiving antenna were conducted such that the antenna is revolved 360° about its vertical axis at a constant angle . This rotation corresponds to a change in angle ψ between the dipole axis of the receiving antenna and the field direction. The angle α is the angle between the direction of the dipole axis of the transmitter antenna and the direction to the receiving point. The measured values obtained by this method are given under U_e in Tables 3 and 4. Column $\bar{U}_e$ was obtained from these values by averaging the measured values belonging to ψ, $\psi + 180°$, $\psi \pm 90°$. The mean values thus obtained are shown in Figs. 6 and 7. The third column gives the mean values $\tilde{U}_e$ calculated by the method of least squares, with allowance for the dependence $U_e = U_{e_0} \cdot \cos \psi$. According to Figs. 6 and 7, this dependence on the angle ψ obviously does not occur, since the minimum of the curve does not assume the value zero, but decreases only down to a certain fraction of the maximum value (see above). In this case, the situation is probably more complex than it was shown by the above theory.

The voltage induced in the antenna calculated according to the law of induction is:

$$| U_{ind} | = \frac{d\phi}{dt} = \frac{d}{dt} \int B \, df \cdot \cos\psi = \frac{d}{dt} \; B \cdot F \cdot \cos\psi \qquad (3)$$

If B is considered to be a constant vector which in the general case may be looked upon as a resultant of the primary field and a series of secondary fields, then it follows from the above equation that the induced voltage becomes zero for the angle $\psi = 90^{\circ}$. Hence, no conclusions can be made from the measured deviation to the disturbing effect of secondary fields caused by the boundary of the ore body.

The most obvious assumption that can still explain the measurement is that of a highly inhomogeneous field. In this case, the situation at the receiving antenna can thus be represented:

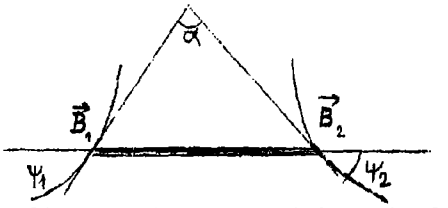

The induced voltage can be represented by the following expression:

$$U_{ind} \sim \vec{B}_1 \cdot \cos\psi_1 + \vec{B}_2 \cdot \cos\psi_2 \qquad (4)$$

The angles ψ_1 and ψ_2 are different owing to the field inhomogeneity and are interrelated (see diagram) in the following way:

$$\psi_1 + \psi_2 + \alpha = 180^{\circ} \qquad (5)$$

This relation can be substituted in (4), α being a measure of the inhomogeneity. From these assumption it follows that the induced voltage need not become zero for whatever value of ψ_1, if the receiving antenna is turned, i.e., if ψ_1 is changed. This is consistent with the actual observation. Here, the effect is explained only qualitatively, not considering the reasons for the great influences on the trans-

mitter field. The following values of the function $\varphi(r, \Delta)$ for 18 and 25 m are calculated from the two measurements:

$\varphi(r,\Delta)$	r(m)
1.15	18
0.75	25

These values are plotted in Fig. 5. The value obtained with good approximation for the conductivity by interpolation is $\sigma \approx 3 \cdot 10^{-1} (\Omega^{-1} m^{-1})$. The error is no more than 25% which considering the small distance is very good. Furthermore, this conductivity is also consistent with that measured with direct current: $2 \cdot 10^{-2} (\Omega^{-1} m^{-1})$.

For a better understanding of Figs. 6 and 7 it must be added that the envelope of all curves gives the field strength diagrams represented in Figs. 1 through 4. The conducted measurements show that $\varphi(r, \Delta) < 1$ for a distance of 25 m, hence measurements for distances of 50 m in the studied rock are already conducted in the far field. This fact is of special interest, since the conditions in the mines of Schwaz and St. Gertraudi are completely different; here, $\varphi(r, \Delta)$ was found to decrease but slightly even at 1000m. For this reason, detailed studies with allowance for the upper and lower boundaries of the ore body can be expected to yield interesting results.

Summary of TN 7

A propagation measurement of VLF waves conducted in the iron ore mine Konrad I (Salzgitter) is discussed in detail and compared with the theory for an unbounded and homogeneous medium. The results of the measurement differ considerably from this simplified theory in some points, which suggests the field to be very inhomogeneous. Furthermore, a representation is given which makes it possible to determine the conductivity of the studied rock by measuring the function $\varphi(r, \Delta)$ which is defined and calculated for a number of r and Δ values.

TABLE I

Calculation of the function

$$h(r,\varphi,\Delta) = \frac{\exp(-\Delta r)}{r}\left\{\frac{4\cos^2\varphi}{r^2}\left(\frac{1}{r^2}+\frac{2\Delta}{r^2}+2\Delta^2\right)+\sin^2\varphi\left(\frac{1}{r^4}+\frac{2\Delta}{r^3}+\right.\right.$$

$$\left.\left.+\frac{2\Delta^2}{r^2}+\frac{4\Delta^2}{r}+4\Delta^2\right)\right\}^{1/2}$$

$$\Delta=\sqrt{\frac{\mu_0\omega\sigma}{2}}$$

f = 3 kc/sec

r	φ	$\Delta = 1.085\cdot10^{-2}$ $\sigma = 10^{-2}(\Omega^{-1}m^{-1})$	$3.45\cdot10^{-2}$ 10^{-1}	$4.86\cdot10^{-2}$ $2\cdot10^{-1}$	$7.7\cdot10^{-2}$ $5\cdot10^{-1}$	$1.09\cdot10^{-1}$ 1
10 m	0	$2\ .10^{-3}$	$1.97.10^{-3}$	$1.9\ .10^{-3}$	$1.79.10^{-3}$	$1.58.10^{-3}$
	30	$1.8\ .10^{-3}$	$1.79.10^{-3}$	$1.73.10^{-3}$	$1.66.10^{-3}$	$1.54.10^{-3}$
	60	$1.31.10^{-3}$	$1.34.10^{-3}$	$1.33.10^{-3}$	$1.38.10^{-3}$	$1.41.10^{-3}$
	90	$9.9\ .10^{-4}$	$1.04.10^{-3}$	1.08.10	$1.22.10^{-3}$	$1.36.10^{-3}$
20 m	0	$2.5\ .10^{-4}$	$2.28.10^{-4}$	$2.08.10^{-4}$	$1.59.10^{-4}$	$1.23.10^{-4}$
	30	$2.26.10^{-4}$	$2.13.10^{-4}$	$2.00.10^{-4}$	$1.65.10^{-4}$	$1.36.10^{-4}$
	60	$1.67.10^{-4}$	$1.78.10^{-4}$	$1.77.10^{-4}$	$1.76.10^{-4}$	$1.6\ .10^{-4}$
	90	$1.27.10^{-4}$	$1.58.10^{-4}$	$1.65.10^{-4}$	$1.81.10^{-4}$	$1.7\ .10^{-4}$
50 m	0	$1.52.10^{-5}$	$9.25.10^{-6}$	$5.6.10^{-6}$	$2.1.10^{-6}$	$6.1\ .10^{-7}$
	30	$1.39.10^{-5}$	$1.01.10^{-5}$	$7.20.10^{-6}$	$3.39.10^{-6}$	$1.31.10^{-6}$
	60	$1.08.10^{-5}$	$1.16.10^{-5}$	$9.60.10^{-6}$	$5.05.10^{-6}$	$2.05.10^{-6}$
	90	$8.90.10^{-6}$	$1.23.10^{-5}$	$1.04.10^{-5}$	$5.70.10^{-6}$	$2.33.10^{-6}$
100 m	0	$1.58.10^{-6}$	$3.56.10^{-7}$	$1.22.10^{-7}$	$1.04.10^{-8}$	$1.55.10^{-9}$
	30	$1.51.10^{-6}$	$5.50.10^{-7}$	$2.38.10^{-7}$	$3.10.10^{-8}$	$6.35.10^{-8}$
	60	$1.42.10^{-6}$	$8.10.10^{-7}$	$3.70.10^{-7}$	$4.94.10^{-8}$	$1.07.10^{-8}$
	90	$1.36.10^{-6}$	$9.66.10^{-7}$	$4.20.10^{-7}$	$5.70.10^{-8}$	$1.24.10^{-8}$
200 m	0	$1.15.10^{-7}$	$2.62.10^{-9}$	$2.17.10^{-10}$	$5.85.10^{-11}$	
	30	$1.37.10^{-7}$	$6.90.10^{-9}$	$7.75.10^{-10}$	$3.32.10^{-10}$	
	60	$1.64.10^{-7}$	$1.13.10^{-8}$	$1.30.10^{-9}$	$5.70.10^{-10}$	
	90	$1.78.10^{-7}$	$1.30.10^{-8}$	$1.50.10^{-9}$	$6.55.10^{-10}$	
500 m	0	$6.06.10^{-10}$	$1.49.10^{-14}$	$1.89.10^{-17}$		
	30	$1.27.10^{-9}$	$9.25.10^{-14}$	$1.60.10^{-16}$		
	60	$2.03.10^{-9}$	$1.59.10^{-13}$	$2.78.10^{-16}$		
	90	$2.32.10^{-9}$	$1.84.10^{-13}$	$3.20.10^{-16}$		

TABLE II

Function $\varphi(r, \Delta)$

r \ Δ	10^{-2}	10^{-1}	$2 \cdot 10^{-1}$	$5 \cdot 10^{-1}$	1
10	2.02	1.93	1.83	1.47	1.16
20	1.97	1.44	1.26	0.88	0.72
50	1.71	0.75	0.54	0.37	0.266
100	1.16	0.37	0.29	0.182	0.125
200	0.65	0.2	0.145	0.09	-
500	0.26	0.081	0.059	-	-

TABLE III

Measurement I
r=18 m

$\vartheta = 0^\circ$

Ψ	U_e	$\bar{U}_e$	$\bar{\bar{U}}_e$
0°	5.3	5.3	5.37
30°	4.5	4.6	4.65
60°	2.5	2.8	2.68
90°	0.85	0.9	0
120°	3.0	2.8	2.68
150°	4.8	4.6	4.65
180°	5.4	5.3	5.37
330°	4.8	4.6	4.65
300°	3.0	2.8	2.68
270°	1.0	0.9	0
240°	2.5	2.8	2.68
210°	4.5	4.6	4.65
0°	5.3	5.3	5.37

$\vartheta = 30^\circ$

Ψ	U_e	$\bar{U}_e$	$\bar{\bar{U}}_e$
30°	5	5	5.16
60°	4.8	4.5	4.46
90°	2.5	3.2	2.58
120°	1.7	1.7	0
150°	2.3	3.2	2.58
180°	4.3	4.5	4.46
210°	5.2	5	5.16
0°	4.2	4.5	4.46
330°	2.4	3.2	2.58

$\vartheta = 60^\circ$

Ψ	U_e	$\bar{U}_e$	$\bar{\bar{U}}_e$
60°	4.7	4.7	4.72
30°	4.2	4.1	4.16
0°	2.7	2.5	2.41
330°	0.8	0.8	0
300°	2.1	2.5	2.41
270°	4.0	4.1	4.16
90°	4.0	4.1	4.16
120°	2.4	2.5	2.41
150°	0.8	0.8	0
180°	2.6	2.5	2.41

$\vartheta = 90^\circ$

Ψ	U_e	$\bar{U}_e$	$\bar{\bar{U}}_e$
270°	4.6	4.6	4.75
60°	4.3	4.3	4.12
30°	2.7	2.5	2.38
90°	4.6	4.6	4.75
120°	4.0	4.3	4.12
150°	2.0	2.5	2.38
180°	0.63	0.6	0
210°	2.7	2.5	2.38
240°	4.3	4.3	4.12

TABLE IV

Measurement II

r = 25 m

$\varphi = 0^\circ$				$\varphi = 30^\circ$			
ψ	U_e	$\bar{U}_e$	$\bar{\bar{U}}_e$	ψ	U_e	$\bar{U}_e$	$\bar{\bar{U}}_e$
0°	2.4	2.4	2.5	0°	2.2	2.2	2.34
30°	2.0	2.2	2.16	30°	2.4	2.4	2.7
60°	1.3	1.6	1.25	60°	2.3	2.2	2.34
90°	0.85	0.85	0	90°	1.8	1.7	1.35
120°	1.6	1.6	1.25	120°	1.5	1.5	0
150°	2.2	2.2	2.16	150°	1.7	1.7	1.35
180°	2.4	2.4	2.5	180°	2.2	2.2	2.34
330°	2.2	2.2	2.16	330°	1.7	1.7	1.35
300°	1.55	1.6	1.25	300°	1.5	1.5	0
270°	0.85	0.85	0				

$\varphi = 60^\circ$				$\varphi = 90^\circ$			
ψ	U_e	$\bar{U}_e$	$\bar{\bar{U}}_e$	ψ	U_e	$\bar{U}_e$	$\bar{\bar{U}}_e$
60°	3.4	3.4	3.3	90°	3.2	3.2	3.18
90°	2.8	2.8	2.85	60°	2.7	2.7	2.74
120°	1.7	1.7	1.65	30°	1.75	1.6	1.59
150°	0.55	0.55	0	0°	1.35	1.3	0
180°	1.6	1.7	1.65	120°	2.7	2.7	2.74
210°	2.8	2.8	2.85	150°	1.6	1.6	1.59
30°	2.8	2.8	2.85	180°	1.3	1.3	0
0°	1.75	1.7	1.65	210°	1.6	1.6	1.59
				240°	2.7	2.7	2.74

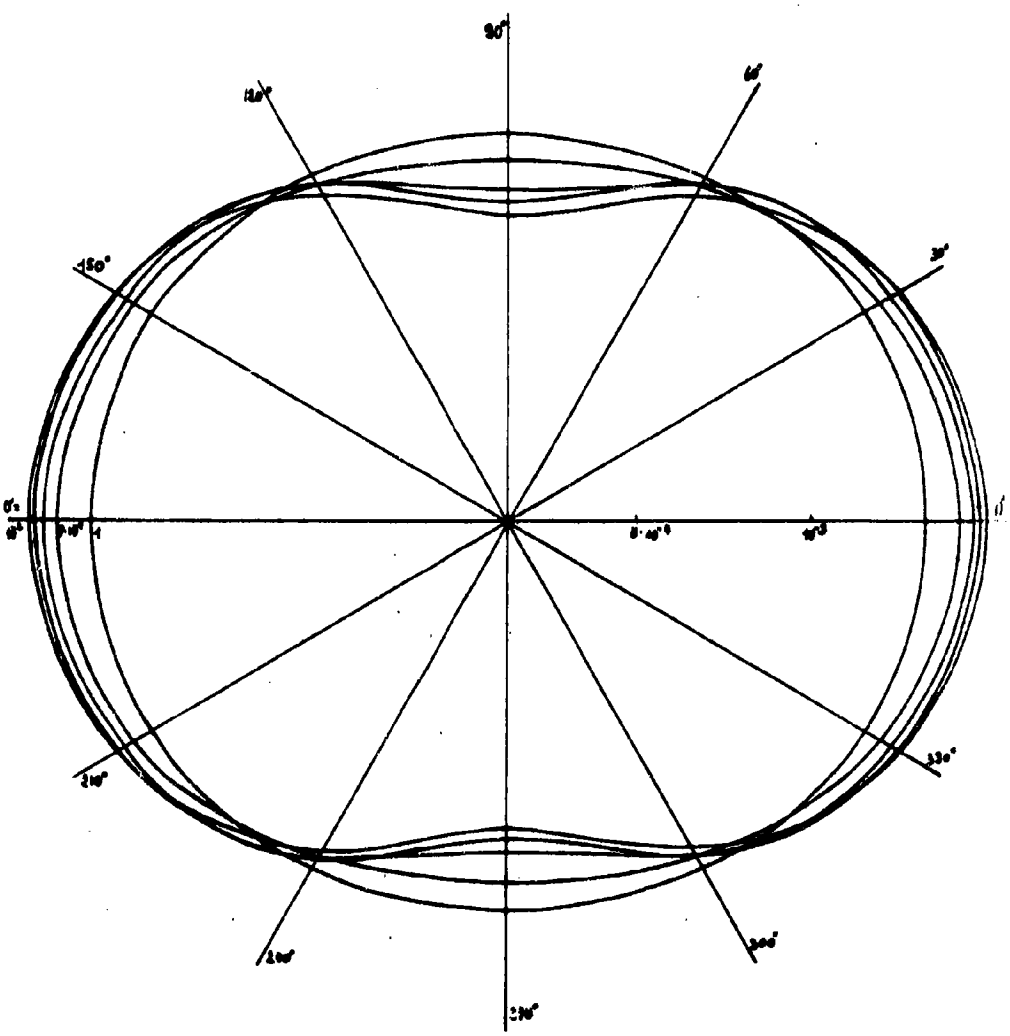

$R(x, \vartheta, \Delta)$

$f = 3\,kc \qquad r = 10m$

Fig. 1

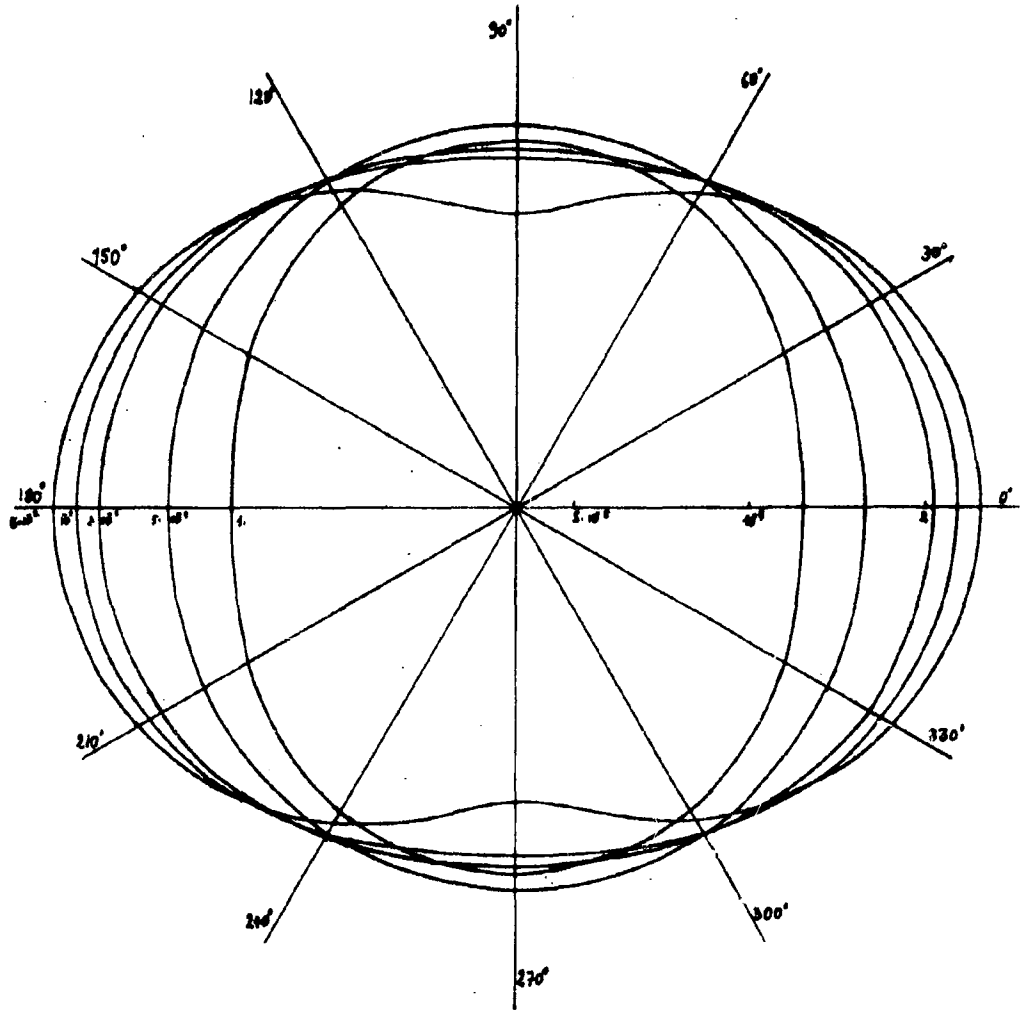

$R(\alpha, \vartheta, \Delta)$
$f = 3\,kHz$ $r = 20\,m$

Fig. 2

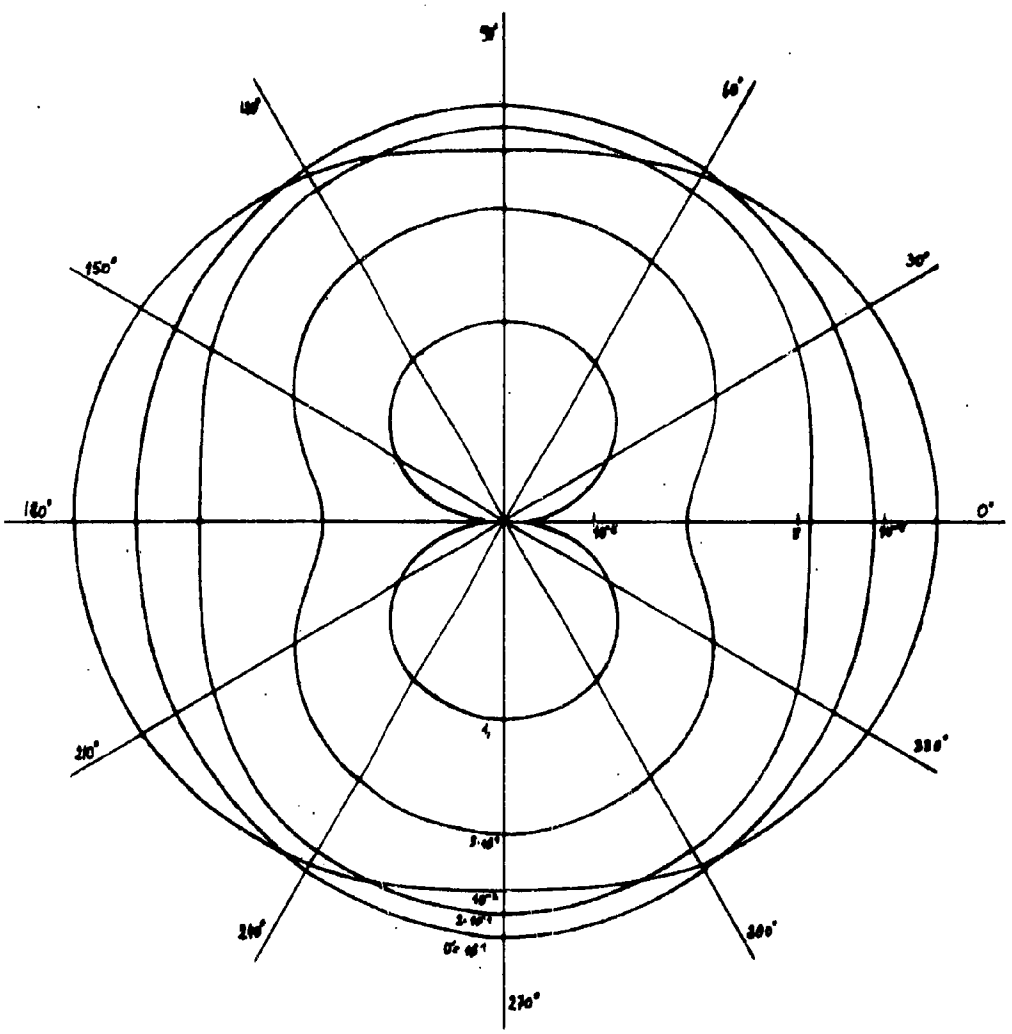

$f(x, \theta, \Delta)$ Fig. 3

$f = 3\,kHz$. $r = 50m$

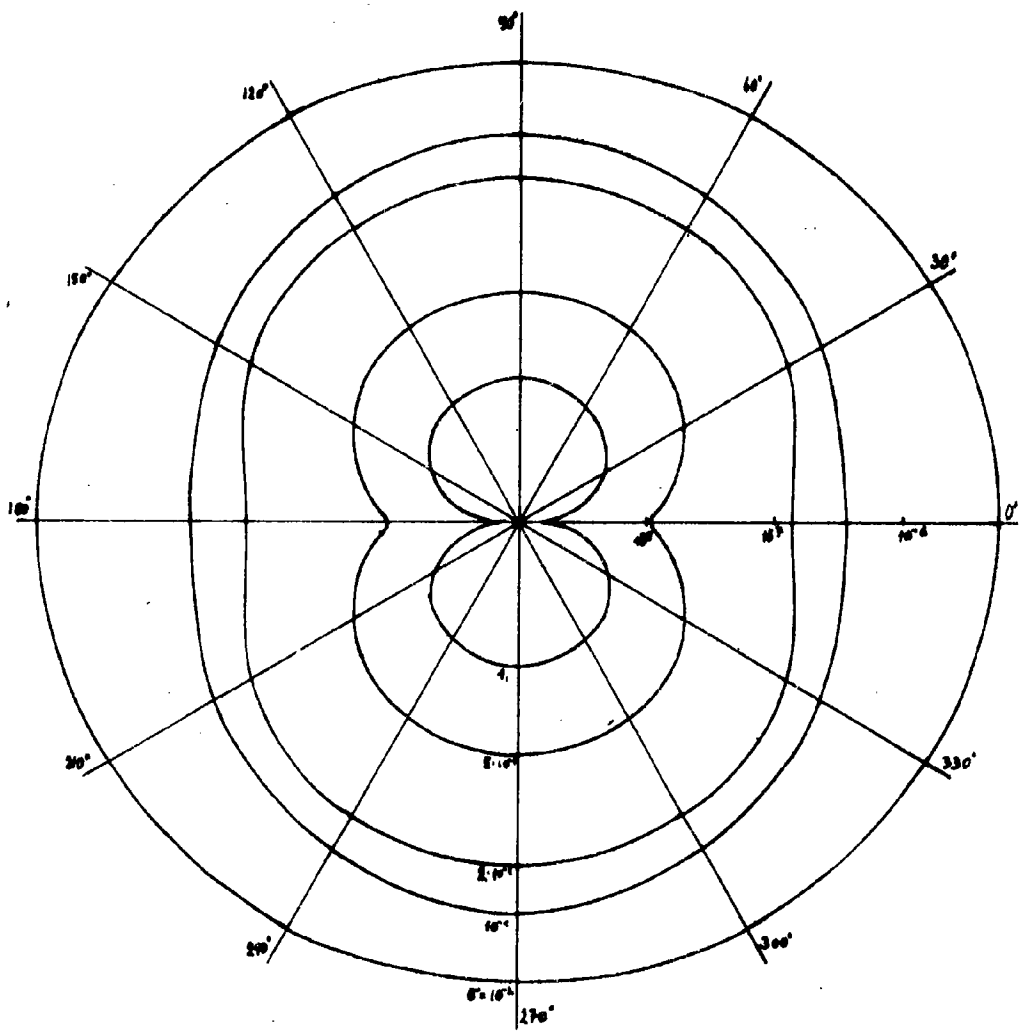

$f(\alpha, \vartheta, \Delta)$
$f = 3\,kc \quad r = 100\,m$

Fig. 4

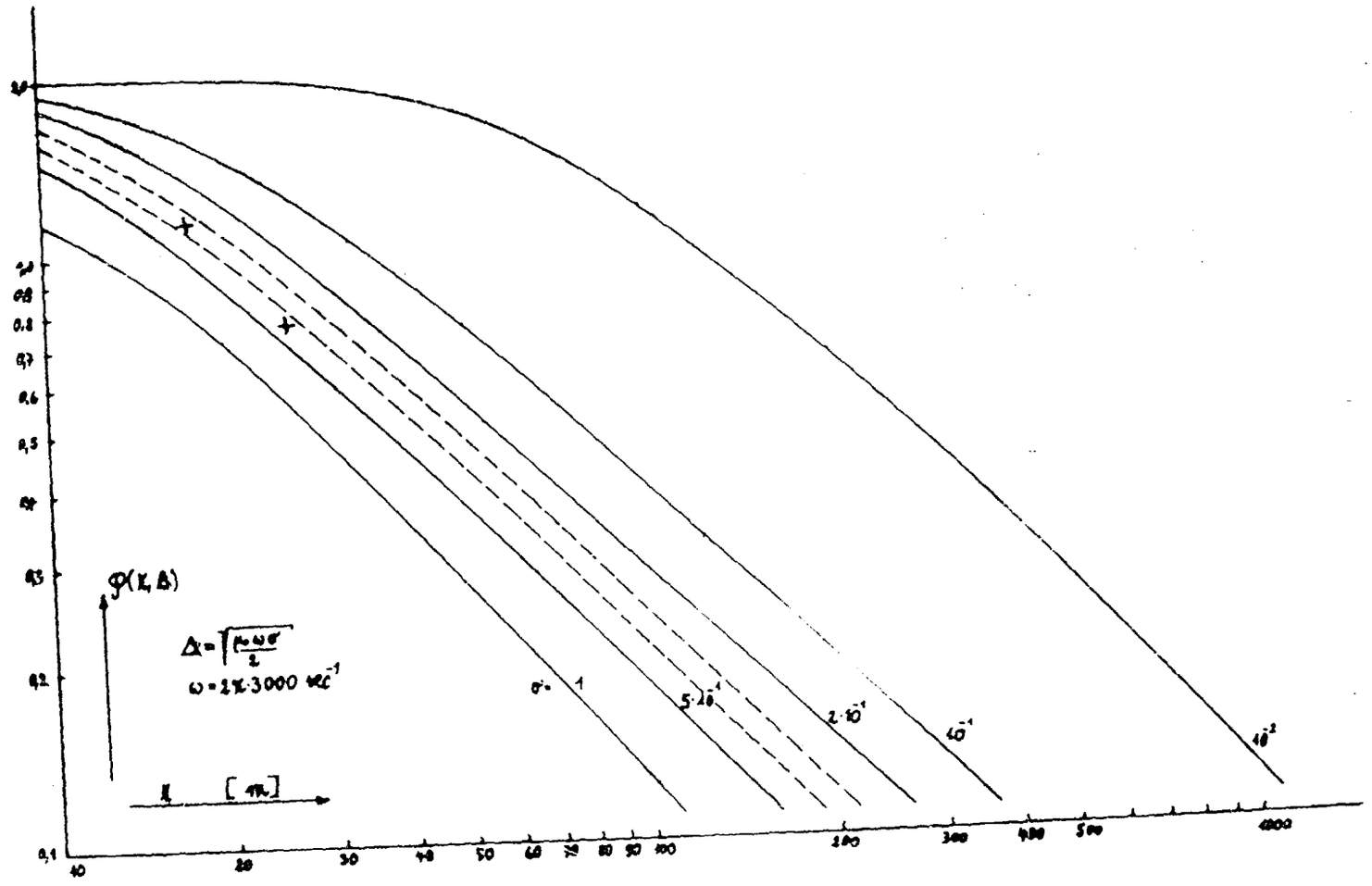

---- INTERPOLATED CURVES

FIG. 5

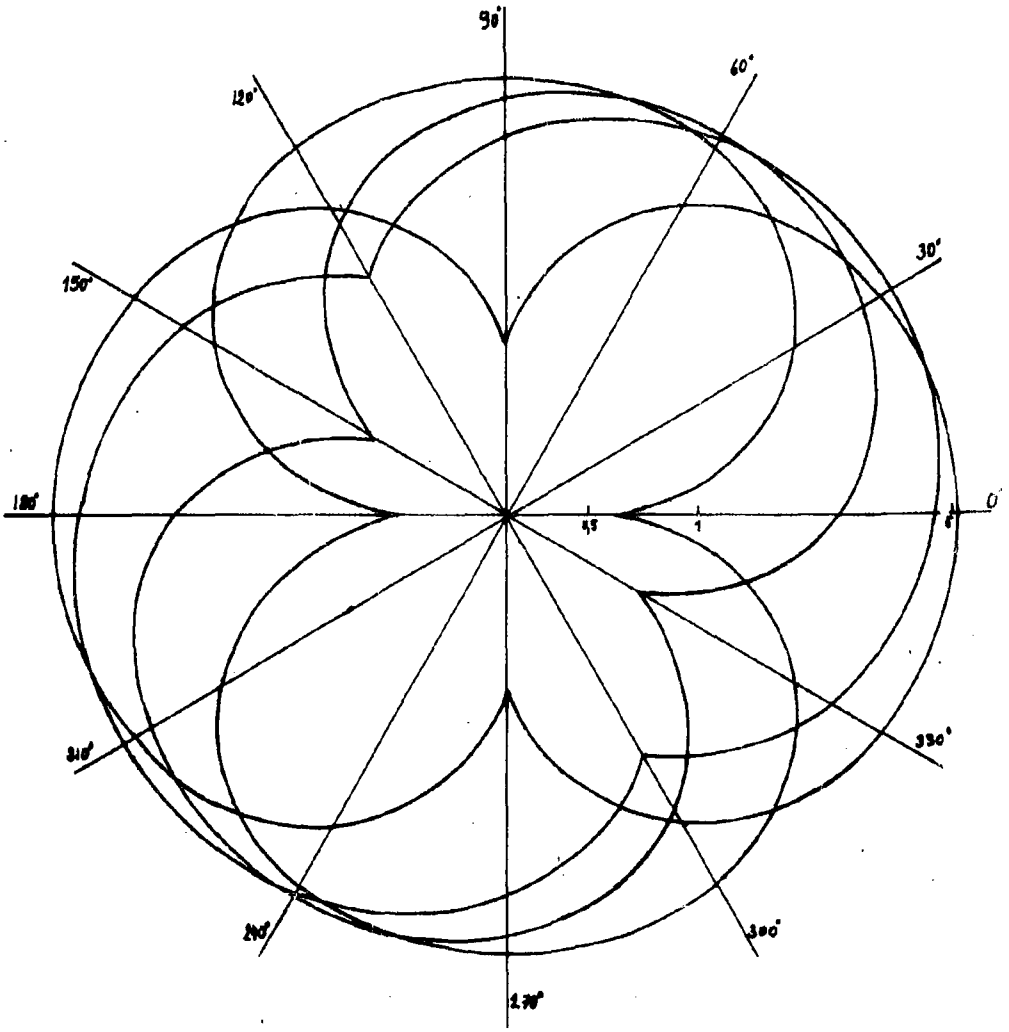

KONRAD I

1. MEASUREMENT

r = 10m f = 3kc

FIG. 6

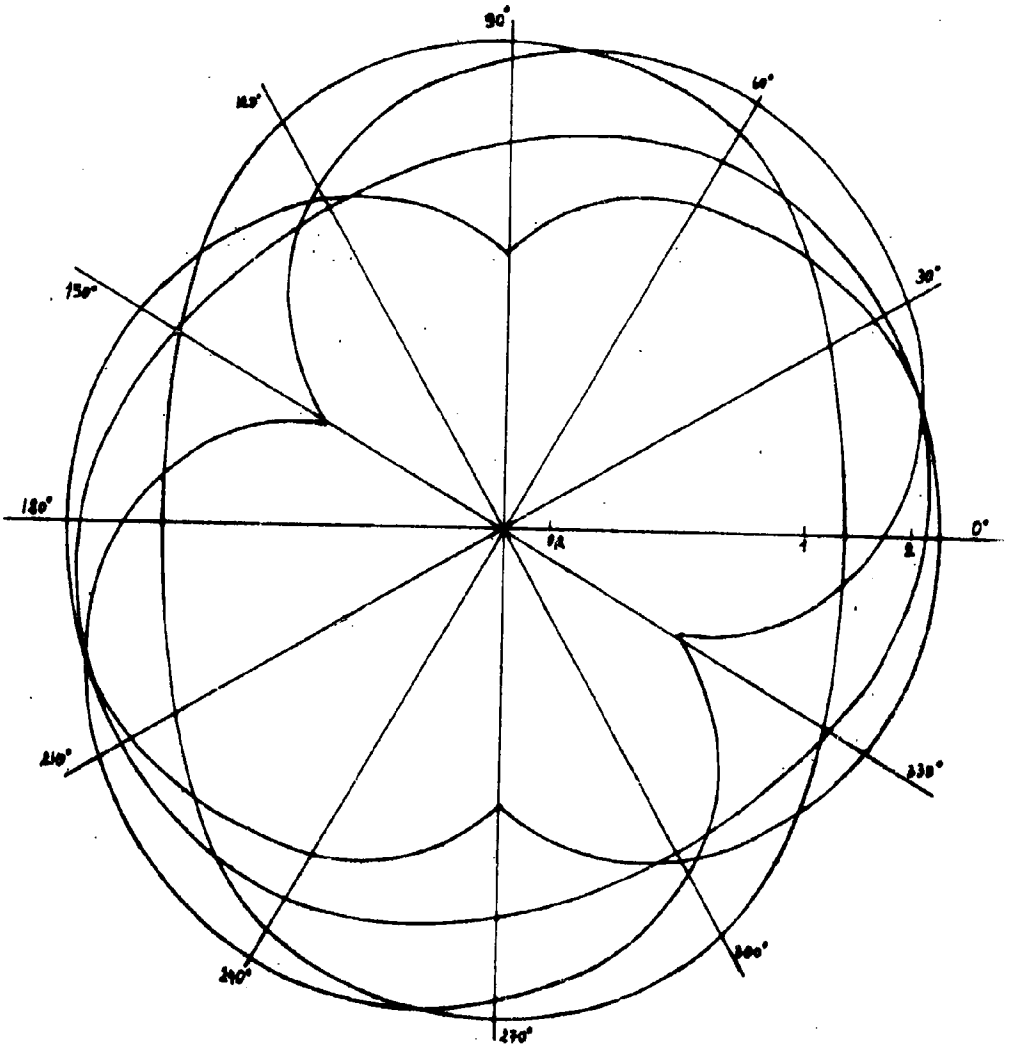

KONRAD I

2. MEASUREMENT

r = 28m f = 3 kc

FIG. 7